Multiple Scattering of Neutrons*

GEORGE H. VINEYARD
Department of Physics, University of Missouri, Columbia, Missouri, and Brookhaven National Laboratory, Upton, New York
(Received June 24, 1954)

The theory of multiple scattering of neutrons is developed in cases of interest for diffraction experiments. Computations of second-order scattering for various plane slab sample arrangements are carried out, under a quasi-isotropic cross-section assumption. The relevance of recent computations by Chandrasekhar is pointed out, and these are also applied to the present problem.

INTRODUCTION

THE determination of crystalline and liquid structures by neutron diffraction depends on measuring single scattering. Higher-order scattering is always present in addition to first-order scattering, and in some cases the experimental data should be corrected accordingly. Although there exists an extensive and elaborate literature on multiple-scattering problems of various types, little of it is exactly applicable to the present situation. Some calculations by Chandrasekhar may be applied in several cases, and these will be considered subsequently. Blok and Jonker[1] have given an approximation method and worked it out numerically in a special application to hydrogenous scatterers. Their method requires rather specific numerical computations for each case, although it permits one to take account of anisotropic cross sections which are not too complicated.

We present in this paper an analysis in terms of orders of scattering. This yields a formal solution to the problem in terms of a sum of definite integrals, and applies to arbitrary sample geometries and for arbitrary scattering cross sections. Evaluation of the early terms of the series is possible for simple geometrical conditions, and gives an adequate approximation whenever the scattering is sufficiently small. The general solution may be used to show certain properties of the scattering, and suggests some approximations which allow one to cope with the very complex cross sections encountered in diffraction problems.

GENERAL ANALYSIS IN TERMS OF ORDERS OF SCATTERING

We consider a sample which consists of a crystalline powder or an amorphous material, so that we can deal exclusively with densities of neutrons instead of Schrödinger waves. We also consider the incident neutrons to be monoenergetic, and neglect the effect of any energy changes during scattering. Let $P_n(\mathbf{r},\mathbf{s})$, $n=0, 1, 2, 3, \cdots$, be defined as the number of neutrons per unit volume at $\mathbf{r}$ which have already been scattered just n times and which are now proceeding in the direction of the unit vector $\mathbf{s}$, within unit solid angle. The scatterer is described by the following parameters:

$\sigma_d(\mathbf{s},\mathbf{s}')$ = differential scattering cross section, per unit volume, for scattering from direction $\mathbf{s}$ to direction $\mathbf{s}'$;

$\sigma=\int\sigma_d d\Omega$ = total scattering cross section per unit volume (here and afterwards $\int d\Omega$ means integration over a solid angle of 4π with respect to the obvious angular variable);

σ_T = total cross section per unit volume (scattering plus absorption).

σ_d is meant to describe the scattering properties of a portion of the material small enough to involve only single scattering, yet large enough to include structural effects, and, in the case of crystalline powders, to contain many crystalline grains representing all orientations. It is thus a macroscopic cross section.

The scattering is governed by a set of transport equations,[2]

$$\mathbf{s}\cdot\nabla P_n(\mathbf{r},\mathbf{s})+\sigma_T P_n(\mathbf{r},\mathbf{s})=\int d\Omega'\sigma_d(\mathbf{s}',\mathbf{s})P_{n-1}(\mathbf{r},\mathbf{s}'),\qquad n=0, 1, 2, \cdots, \tag{1}$$

(where $P_{-1}\equiv 0$) which express the fact that scattering of neutrons of order $n-1$ provides a source, and scattering and absorption of neutrons of order n provide a sink for the current of nth order neutrons at each point $\mathbf{r}$. Equations (1) on the interior of the scatterer, together with boundary conditions prescribing $P_0(\mathbf{r},\mathbf{s})$ at each point of the surface of the scatterer determine all the densities P_n.

A formal set of solutions of Eqs. (1) may be shown to be

$$P_0(\mathbf{r},\mathbf{s})=P_0(\mathbf{r}-L\mathbf{s})\exp(-\sigma_T L), \tag{2a}$$

$$P_n(\mathbf{r},\mathbf{s})=\int d\Omega'\sigma_d(\mathbf{s}',\mathbf{s})\times\int_0^L d\xi\exp(-\sigma_T\xi)P_{n-1}(\mathbf{r}-\xi\mathbf{s},\mathbf{s}'),\qquad n=1, 2, \cdots. \tag{2b}$$

Here L is the distance from the point $\mathbf{r}$ to the surface of the sample in the direction $-\mathbf{s}$. It is assumed that the sample is nowhere concave. See Fig. 1.

* Work carried out under the auspices of the U. S. Atomic Energy Commission.

[1] J. Blok and C. C. Jonker, Physica 18, 809 (1952).

[2] From the basic article by A. M. Weinberg, U. S. Atomic Energy Commission Report AEC-3405 (unpublished) "the derivation of these equations should be evident."

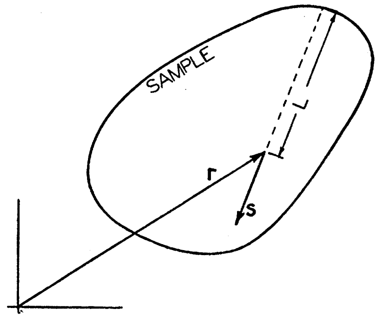

FIG. 1. Geometry of the general case.

Equations (2) state that particles constituting the nth-order component at $\mathbf{r}$ must have suffered their last scattering act somewhere along a line in the direction $-\mathbf{s}$, being at that stage members of the component of order $n-1$, and must then have proceeded to $\mathbf{r}$ without absorption or further scattering.

By iterating Eqs. (2), one can next express P_n as a multiple integral of P_0. In principle the problem is then solved, although the evaluation of these integrals for all but the simplest geometries and cross sections and for $n>2$ proves to be exceedingly tedious. Hereafter, attention will be mainly restricted to samples in the form of a plane slab.

INSTANCE OF THE PLANE SLAB

Suppose the sample to be a slab of indefinite lateral extent and thickness t. Suppose the incoming neutrons to be collimated and incident at an angle θ_0 with the slab normal. For convenience we suppose the incident beam to be of large cross-sectional area, uniformly distributed and containing unit density of neutrons. See Fig. 2.

The neutron densities now become functions of z, the depth below the surface, and θ, the direction of the vector $\mathbf{s}$. We find from Eqs. (2),

$$P_0(z,\theta)=\exp(-\sigma_T z\sec\theta_0)(2\pi)^{-1}\delta(\cos\theta-\cos\theta_0), \quad (3)$$

and

$$P_1(z,\theta)=\sigma_d(\mathbf{s},\mathbf{s}_0)\left[\frac{\exp(-\sigma_T z\sec\theta_0)}{\sigma_T\cos\theta}\right]\times\left[\frac{\exp[\sigma_T L(\sec\theta_0\cos\theta-1)]-1}{\sec\theta_0-\sec\theta}\right], \quad (4)$$

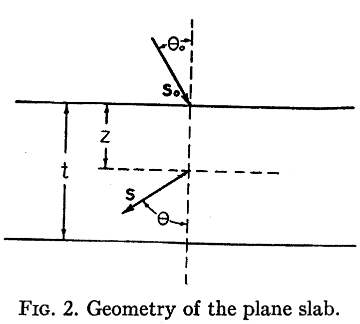

FIG. 2. Geometry of the plane slab.

where

$$L=z\sec\theta,\quad \theta<\pi/2;\quad L=(z-t)\sec\theta,\quad \theta>\pi/2, \quad (5)$$

and δ indicates the Dirac δ function. At the bottom of the slab, (4) gives, with $\sigma_T t=\tau$,

$$P_1(t,\theta)=\sigma_d(\mathbf{s},\mathbf{s}_0)\left[\frac{\exp(-\tau\sec\theta_0)}{\sigma_T\cos\theta}\right]\times\left[\frac{\exp[\tau(\sec\theta_0-\sec\theta)]-1}{\sec\theta_0-\sec\theta}\right],\quad \theta<\pi/2, \quad (6)$$

and at the top,

$$P_1(0,\theta)=\sigma_d(\mathbf{s},\mathbf{s}_0)\left[\frac{\exp[-\tau(\sec\theta_0-\sec\theta)]-1}{\sigma_T\cos\theta(\sec\theta_0-\sec\theta)}\right],\quad \theta>\pi/2. \quad (7)$$

To calculate the current density in nth-order scattering which leaves the surface of the slab, it is only necessary to multiply P_n, evaluated at the surface, by the velocity of the neutrons. The current is the current density multiplied by the cross-sectional area of the beam, and if $J_n(\theta)$ is the nth-order scattered current, per unit incident current, transmitted through the slab at direction θ, per unit solid angle, we find

$$J_n(\theta)=(\cos\theta/\cos\theta_0)P_n(t,\theta),\quad n=0,1,2,\cdots. \quad (8)$$

In the following, second-order scattering will be computed for three specific cases:[3] (a) angle of incidence equal to angle of transmission, (b) angle of incidence equal to zero, and (c) reflection at an angle equal to angle of incidence, sample infinitely thick.

Case (a): $\theta=\theta_0$

Equation (2b), with $n=2$, applied to Eq. (4) gives

$$P_2(t,\theta)=\sigma_T^{-2}\sec\theta e^{-\tau\sec\theta}\int d\Omega'\sigma_d(\mathbf{s},\mathbf{s}')\sigma_d(\mathbf{s}',\mathbf{s}_0)f(\theta'), \quad (9)$$

where $\mathbf{s}'$ is a unit vector making angle θ' with the (downward) slab normal, and

$$f(\theta')=\frac{|\sec\theta'|}{(\sec\theta-\sec\theta')^2}\{\exp[\tau|\sec\theta'|(\sec\theta\cos\theta'-1)]-1\}-\frac{\tau\sec\theta'}{\sec\theta-\sec\theta'}.$$

In general, this integral can be handled only by numerical methods. However, for most liquid and crystalline

[3] With the quasi-isotropic approximation it does not matter (in second- and higher-order scattering) whether the direction of emergence is co-planar with the slab normal and the direction of incidence. In developing the δ-function approximation this further restriction will be assumed.

samples, σ_d is a rapidly varying function of angle which, if averaged over a small range of angles about any angle, would be virtually a constant, equal to $\sigma/4\pi$. $f(\theta')$ is a relatively slowly varying function, and we thus find that a good approximation to P_2 is given by replacing the two differential cross sections by $\sigma/4\pi$ and removing them from the integral. This approximation is inadequate for θ very small, or for the case of x-ray scattering where, at not too long wavelengths, the atomic structure factor imparts a pronounced secular trend to σ_d. We call it the quasi-isotropic approximation.

With the quasi-isotropic approximation the integral in (9) may be evaluated, to give:

$$J_2(\theta)=P_2(t,\theta)=\left(\frac{\sigma}{\sigma_T}\right)^2\frac{e^{-\tau s}}{8\pi s}\Big[\left(\frac{s}{s-1}\right)(1-e^{(s-1)\tau})$$
$$+(s\tau+1)\{\overline{\mathrm{Ei}}([s-1]\tau)-\ln([s-1]\tau)\}$$
$$+\left(\frac{s}{s+1}\right)(1-e^{-(s+1)\tau})+(1-s\tau)$$
$$\times\{\mathrm{Ei}(-[s+1]\tau)-\ln([s+1]\tau)\}+2\ln\tau$$
$$-(e^{s\tau}+e^{-s\tau})\,\mathrm{Ei}(-\tau)\Big], \quad (10)$$

where $s=\sec\theta$,

$$\mathrm{Ei}(x)=\int_{-\infty}^{x}\frac{e^u}{u}du, \quad x<0,$$

and $\overline{\mathrm{Ei}}(x)$ is defined by the same integral as $\mathrm{Ei}(x)$, with $x>0$; the integral is understood in the sense of the Cauchy principal value.[4]

There is another form of σ_d, the δ function approximation, which allows rather simple evaluation of (9) and which approximates a variety of situations, including both isotropic and highly anisotropic examples. Let

$$\sigma_d(\chi)=\sum_{n=1}^{N}a_n\delta(\chi-b_n), \quad (11)$$

where χ is the scattering angle, and a_n and b_n are arbitrary. This form is well suited to the cross section of a crystalline powder, for example. Let the pole of a spherical coordinate system coincide with the downward slab normal. Let $\mathbf{s}$, $\mathbf{s}_0$, and the slab normal be co-planar. Let $\mathbf{s}'$ have polar angles θ' and φ', where φ' is measured from the plane of $\mathbf{s}$ and $\mathbf{s}_0$. Let the angle between $\mathbf{s}'$ and $\mathbf{s}_0$ be η, between $\mathbf{s}'$ and $\mathbf{s}$ be ζ. One finds, assuming $\theta=\theta_0$, $(\chi=2\theta)$,

$$\cos\eta=\cos\theta'\cos\theta-\sin\theta'\sin\theta\cos\varphi',$$
$$\cos\zeta=\cos\theta'\cos\theta+\sin\theta'\sin\theta\cos\varphi',$$
$$\theta'=\cos^{-1}[(\cos\eta+\cos\zeta)/2\cos\theta].$$

The solid angle $d\Omega'$ can be written: (when $\theta\neq0$)

$$d\Omega'=\sin\theta' d\theta' d\varphi'=I(\eta,\zeta)d\eta d\zeta, \quad (12)$$

where

$$I(\eta,\zeta)=\left[1-\left(\frac{\cos2\theta-\cos\eta\cos\zeta}{\sin\eta\sin\zeta}\right)^2\right]^{-\frac{1}{2}}.$$

Inserting (11) and (12) in (9), we find

$$P_2(t,\theta)=\sigma_T^{-2}\sec\theta e^{-\tau\sec\theta}\times\sum_{n=1}^{N}\sum_m{}^* a_na_mI(b_n,b_m)f(\theta_{nm}'), \quad (13)$$

where θ_{nm}' means θ' at $\eta=b_n$, $\zeta=b_m$, and $\sum_m{}^*$ means summation over all m for which $|b_n-2\theta|\le b_m\le|b_n+2\theta|$.

Equation (13) can be explicitly evaluated without much trouble for reasonable values of N. From its form one sees that the peaks in σ_d do not appear directly in J_2. The individual terms of (13) are not monotonic in θ, however, since $I(b_n,b_m)$ becomes infinite when $2\theta=|b_n\pm b_m|$. The resulting infinities in P_2 are caused by the infinitely sharp peaks assumed for σ_d. Allowing a small but finite width w (radians) for each peak of σ_d, and keeping the areas of each peak unchanged, one finds that at these infinities one should replace $I(b_n,b_m)$ in (13) by

$$[(9/32)|\cot b_n\pm\cot b_m|w]^{-\frac{1}{2}},$$

corresponding to the cases $|b_n\pm b_m|=2\theta$, respectively. Correction of I is unnecessary whenever $2\theta-|b_n\pm b_m|\gg w$.

For $w=0.01$ radian, $b_n=80°$, $b_m=90°$, this gives a peak only about 4 times as high as the minimum point on the curve of $I(b_n,b_m)$ vs θ. Thus, in typical crystalline cases these peaks are low and broad, and the superposition of all of them leads to a rather smooth curve resembling that of the quasi-isotropic approximation.

Case (b): $\theta_0=0$

A precisely similar calculation, again making the quasi-isotropic approximation, reveals that

$$J_2(\theta)=\cos\theta P_2(t,\theta)=\left(\frac{\sigma}{\sigma_T}\right)^2\frac{e^{-\tau s}}{8\pi}$$
$$\times\Big[-\frac{1}{s}(e^{\tau s}+e^{-\tau})\,\mathrm{Ei}(-\tau)+\frac{1}{s-1}\mathrm{Ei}(-2\tau)$$
$$-\frac{1}{s(s-1)}e^{\tau(s-1)}\,\mathrm{Ei}(-\tau[s+1])-\frac{1}{s(s-1)}$$
$$\times\{\overline{\mathrm{Ei}}(\tau[s-1])-\ln(\tau[s-1])+\ln\tau\}$$
$$+\frac{1}{s-1}e^{\tau(s-1)}\ln(\tfrac{1}{2}\gamma\tau)+\frac{1}{s(s-1)}$$
$$\times e^{\tau(s-1)}\ln(s+1)+\left(\frac{e^{\tau(s-1)}-1}{s-1}\right)\ln2\Big], \quad (14)$$

[4] E. Jahnke and J. Emde, *Table of Functions* (G. E. Stechert and Company, New York, 1938), pp. 1–3. A. Hammad, Phil. Mag. **38**, 515 (1947).

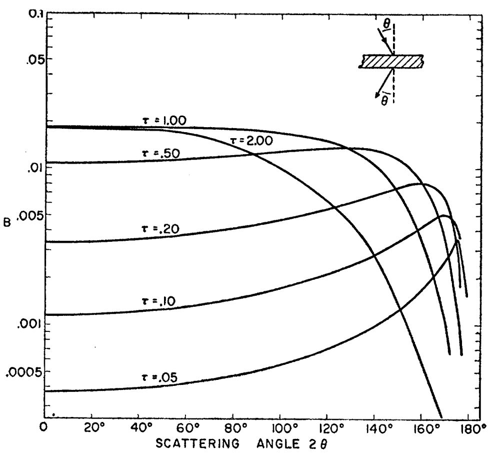

FIG. 3. Second scattering coefficient, B *vs* scattering angle, 2θ [case (a)].

where $\gamma = 1.78107\cdots$.

Case (c): Reflection at the Specular Angle, Thick Slab

This is the only case giving simple results. With the same procedure, and the quasi-isotropic approximation, we find

$$J_2(\theta) = P_2(0,\theta) = (\sigma/\sigma_T)^2(8\pi\sec\theta)^{-1}\ln(1+\sec\theta). \quad (15)$$

Here, contrary to the previous convention, θ has been measured from the upward normal, as pictured in Fig. 4.

Summary of Plane Slab Results

In all three cases, we find that the first- and second-order scattered currents can be written, respectively,

$$J_1 = (\sigma/\sigma_T)A4\pi\sigma_d(\chi)/\sigma, \quad (16)$$

$$J_2 = (\sigma/\sigma_T)^2 B, \quad (17)$$

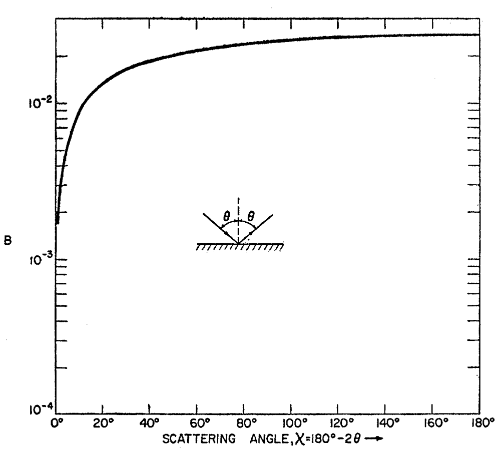

FIG. 4. Case (c) (back reflection) second scattering coefficient, B *vs* scattering angle, $\pi - 2\theta$.

where A and B may be called the first- and second-order scattering coefficients, and are defined by Eqs. (10), (14), and (15) in conjunction with the preceding expressions. The angle χ is the scattering angle, equal to 2θ, θ, and $\pi-2\theta$, in cases (a), (b), and (c), respectively. Equation (16) has been cast into such a form that the mean value of the differential cross-section dependent factor, $4\pi\sigma_d(\chi)/\sigma$, is unity. A and B each depend on τ and $\sec\theta$ only.

Equations (16) and (17) indicate at once the role of the ratio σ/σ_T, which may be termed an "albedo," in fixing the magnitude of the various orders of scattering. One may further show, by a simple change of variables in the second integral of Eq. (2b), that P_n is quite generally proportional to $(\sigma/\sigma_T)^n$. From this it is clear that a sufficiently large absorption cross section can always reduce higher-order scattering indefinitely compared to first order scattering. With x-rays the albedo is typically from 0.1 to 0.01 and thus multiple scattering corrections are generally less important for x-rays than for neutrons.

The second scattering coefficient B (under the quasi-isotropic approximation) is plotted *vs* the scattering angle χ in Figs. 3 and 4, for cases (a) and (c), respectively. In Fig. 3, various values of the thickness parameter τ lead to the various curves. Here, a tendency of second-order scattering to be isotropic is apparent, especially for τ in the vicinity of 1.

In Fig. 5 is plotted the ratio of second-order scattering coefficient B to first-order coefficient A, for case (a), with quasi-isotropic approximation. The thickness parameter τ is abscissa. For modest scattering angles the ratio is nearly independent of scattering angle. From the curves, one sees that τ must be as small as 0.05 to make B/A equal $\frac{1}{10}$. With vanishing thickness, the ratio vanishes, but as $\tau\ln\tau$, rather than linearly with τ, as one might have at first supposed.

LIMITS OF VALIDITY OF THE RESULTS

The implicit assumption of the foregoing work has been that second-order scattering forms such a large share of the multiple scattering that third, fourth, etc., orders may be ignored. This assumption is valid only under special circumstances. Rough calculation shows that third-order scattering is about as much smaller than second order as second order is smaller than first, and this proportion extends to all higher orders as well. Consequently, if second-order scattering is much less than first order, we may generally conclude that second order is well representative of all higher orders. Two conditions, as has been noted, favor this: smallness of τ, and smallness of the albedo, σ/σ_T. From the curves given here one can immediately determine whether this condition is satisfied.

To demonstrate more fully the relative magnitudes of the various higher orders of scattering, suitable relations of inequality can be found. Define

$$Q_n(\mathbf{r})=\int d\Omega P_n(\mathbf{r},\mathbf{s}), \tag{18}$$

the nth-order neutron density at $\mathbf{r}$. With the quasi-isotropic approximation, Eq. (2b) may be rewritten

$$P_n(\mathbf{r},\mathbf{s})=(\sigma/4\pi)\int_0^L d\xi\, \exp(-\sigma_T\xi)Q_{n-1}(\mathbf{r}-\xi\mathbf{s}).$$

Now if the maximum value of $Q_n(\mathbf{r})$, for all $\mathbf{r}$, is denoted $Q_n^{\max}$, we have

$$P_n(\mathbf{r},\mathbf{s})\leq(\sigma/4\pi)Q_{n-1}^{\max}\int_0^L d\xi\, \exp(-\sigma_T\xi)$$
$$=(\sigma/4\pi\sigma_T)Q_{n-1}^{\max}[1-\exp(-\sigma_T L)]. \tag{19}$$

Specializing now to the plane slab case, L is given by Eq. (5). Next, integrate Eq. (19) with respect to the solid angle associated with $\mathbf{s}$. One finds

$$Q_n(\mathbf{r})\leq(\sigma/\sigma_T)[1-F(z)]Q_{n-1}^{\max},$$

TABLE I. Test of approximations.

σ/σ_T	τ	Error in using J_2	Error in using Eq. (23)
1	0.1	−20%	−4%
1	0.5	−45%	+5%
0.5	0.5	−21%	+1.5%

where

$$F(z)=\tfrac{1}{2}\{\exp[-\sigma_T z]+\exp[-\sigma_T(t-z)]$$
$$+\sigma_T z\, \mathrm{Ei}(-\sigma_T z)+\sigma_T(t-z)\, \mathrm{Ei}[-\sigma_T(t-z)]\}.$$

The minimum value of $F(z)$ occurs at $z=t/2$, so finally,

$$Q_n^{\max}\leq(\sigma/\sigma_T)g(\tau)Q_{n-1}^{\max}, \tag{20}$$

where

$$g(\tau)=1-F(t/2)$$
$$=1-\exp(-\tau/2)-(\tau/2)\,\mathrm{Ei}(-\tau/2). \tag{21}$$

$g(\tau)$ is plotted in Fig. 6.

Iterating the inequalities (20), we find

$$Q_n^{\max}\leq[(\sigma/\sigma_T)g(\tau)]^{n-m}Q_m^{\max}. \tag{22}$$

The general level of higher than second-order scattering cannot exceed $\sum_{n=3}^{\infty} Q_n^{\max}$; so by (22), this level cannot exceed

$$\sum_{n=3}^{\infty}[(\sigma/\sigma_T)g(\tau)]^{n-2}Q_2^{\max}$$
$$=Q_2^{\max}[(\sigma/\sigma_T)g(\tau)][1-(\sigma/\sigma_T)g(\tau)]^{-1}.$$

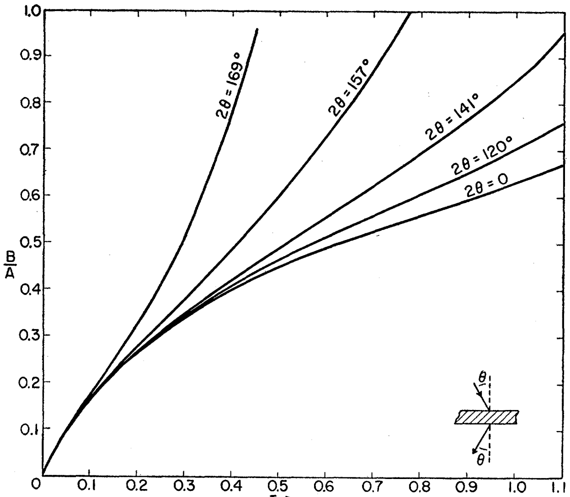

FIG. 5. Ratio of 2nd to 1st scattering coefficients, B/A vs τ [case (a)].

From this it is clear that smallness of $(\sigma/\sigma_T)g(\tau)$ compared to unity insures that second-order scattering is a close approximation to all of the multiple scattering. Comparison of Fig. 6 and Fig. 5 shows that this criterion is nearly the same as the previously described criterion that $(\sigma/\sigma_T)(B/A)$ be small.

From these calculations a rough tendency for the ratio J_{n+1}/J_n to be independent of n is apparent. This suggests an improved approximation for the multiple scattering. Assume $J_{n+1}/J_n=J_2/\bar{J}_1$, $n=2, 3, \cdots$, where $\bar{J}_1$ means the average of J_1 over angles. Employing (16) and (17), we have $J_2/\bar{J}_1=(\sigma/\sigma_T)(B/A)$. Then

$$J_2+J_3+J_4+\cdots\cong J_2[1+(\sigma/\sigma_T)(B/A)$$
$$+(\sigma/\sigma_T)^2(B/A)^2+\cdots],$$

or

$$J_2+J_3+J_4+\cdots\cong J_2/[1-(\sigma/\sigma_T)(B/A)]. \tag{23}$$

Equation (23) is an appreciable improvement over J_2 itself, as long as $(\sigma/\sigma_T)(B/A)<1$. A test of this is afforded by Chandrasekhar's exact calculation for isotropic scattering [case (b)]. For $\theta=0$, one finds errors as listed in Table I.

CHANDRASEKHAR'S COMPUTATIONS

The problem of multiple scattering without energy loss has already had considerable attention from

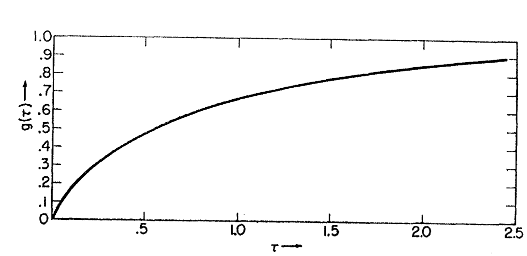

FIG. 6. $g(\tau)$ vs τ, plane slab case [see Eq. (21)].

astrophysicists, to whom it is of interest in connection with problems of radiative equilibrium in stellar and planetary atmospheres. Chandrasekhar[5,6] has shown that the total scattering (all orders) for plane-slab scatterers with isotropic cross section is determined by two functions satisfying integral equations which, though nonlinear, are adapted to numerical computation. He and co-workers have recently published tabulations of these basic functions.[7]

Within the realm covered by the published tabulations, and after justification of the quasi-isotropic approximation, this work is clearly superior to an analysis in terms of orders of scattering. Its advantages are especially great for cases of thick scatterers. There is the disadvantage that the scattered intensity appears as the ratio of certain differences of the tabulated functions and the quantity $\cos\theta_0 - \cos\theta$, where θ_0 and θ are incident and emergent angles, respectively. For the case most important in neutron diffraction [our case (a)] this ratio is 0/0, and the limit as θ approaches θ_0 cannot be found with accuracy from the tabulated values.[8]

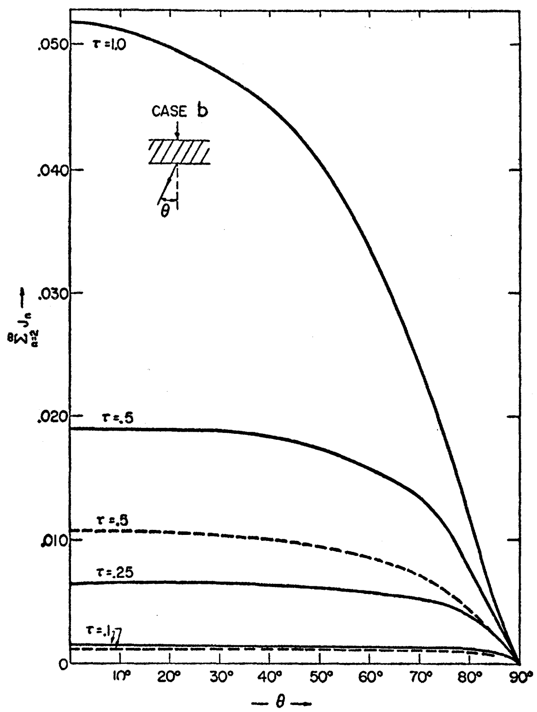

FIG. 7. Multiple scattering, $\Sigma_{n=2}^{\infty} J_n$, from Chandrasekhar. $\sigma/\sigma_T=1$ [dotted lines give J_2, (Eq. (14)].

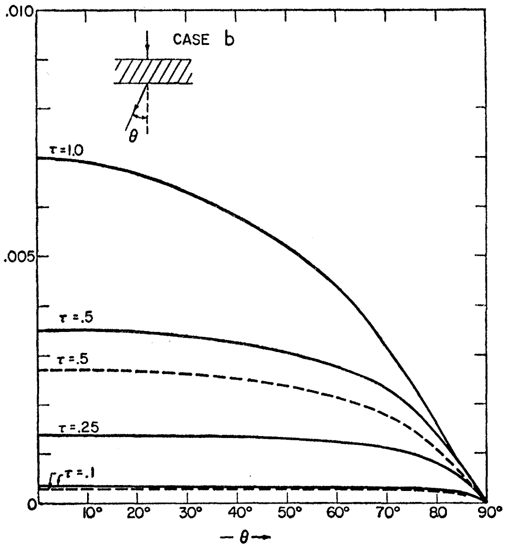

FIG. 8. Multiple scattering, $\Sigma_{n=2}^{\infty} J_n$, from Chandrasekhar. $\sigma/\sigma_T=0.5$ [dotted lines give J_2, Eq. (14)].

We have employed Chandrasekhar's tables to compute multiple scattering in our case (b), where, for the parameter ranges tabulated they are superior to our Eq. (14). Computing J_1 from Eqs. (4) and (8), we subtract this from the Chandrasekhar values (which give $\sum_{n=1}^{\infty} J_n$), and present the results in Figs. 7 and 8. Again the approximate isotropy for angles which are not too large can be seen, particularly for thin samples.

Also plotted in Figs. 7 and 8 are curves of J_2, computed from Eq. (14) for $\tau=0.1$ and $\tau=0.5$. Qualitatively, the second-order curves are entirely similar to the curves which include all higher orders. For $\tau=0.5$, $\sigma/\sigma_T=1$, the quantitative agreement is poor, for the other cases it is fair to good, as has been predicted by the foregoing considerations.

ACKNOWLEDGMENTS

The writer is indebted to D. A. Kleinman for valuable suggestions, to Miss Jean Snover for a great deal of help with the computations, to S. Chandrasekhar for comments, and to the Brookhaven National Laboratory for its hospitality during the course of this work.

[5] S. Chandrasekhar, *Radiative Transfer* (Clarendon Press, Oxford, 1950), Chap. IX.

[6] A multiple-scattering treatment somewhat similar to that presented here, but not carried beyond the abstract stage, has also been given by H. C. van de Hulst, Astrophys. J. **107**, 220 (1948).

[7] Chandrasekhar, Elbert, and Franklin, Astrophys. J. **115**, 244, 269 (1952).

[8] Chandrasekhar has also given analytic approximations to his two functions (reference 5, pages 202–207), and from these one can treat the case $\theta=\theta_0$ with an accuracy comparable to that of the present work. The formulas seem to be more cumbersome, however.